International Journal of Nanomedicine

Dovepress
open access to scientific and medical research

Open Access Full Text Article

ORIGINAL RESEARCH

Multifunctional folate receptor-targeting and pH-responsive nanocarriers loaded with methotrexate for treatment of rheumatoid arthritis

This article was published in the following Dove Press journal:
International Journal of Nanomedicine
11 September 2017
Number of times this article has been viewed

Jinlong Zhao[1]
Menghui Zhao[1]
Changhui Yu[1]
Xueyan Zhang[1]
Jiaxin Liu[1]
Xinwei Cheng[2]
Robert J Lee[1,2]
Fengying Sun[1]
Lesheng Teng[1]
Youxin Li[1]

[1]School of Life Sciences, Jilin University, Changchun, China; [2]College of Pharmacy, Ohio State University, Columbus, OH, USA

Abstract: Rheumatoid arthritis (RA) is an autoimmune disease characterized by progressive cartilage and bone destruction. Activated macrophages that overexpress folic acid (FA) receptors play an important role in RA, due to their abundance in inflamed synovial membrane and joints. In an effort to deliver drugs to the inflamed tissues, multifunctional FA receptor-targeting and pH-responsive nanocarriers were developed. They were composed of lipids, polyethylene glycol (PEG)–poly(lactic-*co*-glycolic acid) (PLGA) forming a hydrophilic shell, FA around the hydrophilic shell as a targeting ligand, and poly(cyclohexane-1,4-diylacetone dimethylene ketal) (PCADK) and PLGA as a hydrophobic core. PCADK also acts as a pH-responsive material. Methotrexate (Mtx) was encapsulated in the nanoparticles, which exhibited pH-responsive release in vitro. Cellular uptake and cytotoxicity experiments revealed that FA-PEG-PLGA/PCADK–lipid nanoparticles loaded with Mtx (FA-PPLNPs) exhibited superior cellular uptake and higher cytotoxicity to activated macrophages than PPLNPs/Mtx. The therapeutic effect of FA-PPLNPs/Mtx in RA was confirmed in an adjuvant-induced arthritis rat model. These results suggest that the multifunctional folate receptor-targeting and pH-responsive nanocarriers are promising for the treatment of RA.

Keywords: rheumatoid arthritis, methotrexate, nanoparticles, folate, pH-responsive, PCADK

Introduction

Rheumatoid arthritis (RA) is an autoimmune disease that is associated with progressive cartilage and bone destruction.[1,2] It affects a large fraction of the aging population and can cause severe pain and disability.[3] However, the exact mechanism of RA is not clear.[4] Macrophages play a vital role in RA, due to their high abundance in diseased synovial membrane and joints.[4–7] Among receptors that are overexpressed on activated macrophages is FRβ.[8] Methotrexate (Mtx) is an antirheumatic drug that has been used for treatment of RA in the clinic for decades.[9] Mtx is frequently used in combination with other biologic agents.[10–12] However, long-term use and high-dose Mtx given by systematic administration have been associated with drug resistance and adverse side effects.[13,14] Therefore, it is desirable to develop a system that can deliver Mtx selectively to target tissues and to release the encapsulated Mtx within a short time.[15]

Recently, hybrid lipid–polymer nanoparticles (LPNPs) have been studied extensively for drug delivery in many diseases.[16–19] Characteristics of LPNPs include high biocompatibility and prolonged circulation in the bloodstream.[20] LPNPs can selectively accumulate at tumor tissues as a result of the enhanced permeation-and-retention effect.[21]

Correspondence: Lesheng Teng; Youxin Li
School of Life Sciences, Jilin University, 2699 Qianjin Street, Changchun, Jilin 130012, China
Tel/fax +86 431 8515 5320
Email tenglesheng@jlu.edu.cn; liyouxin@jlu.edu.cn

submit your manuscript | www.dovepress.com
Dovepress
http://dx.doi.org/10.2147/IJN.S140992

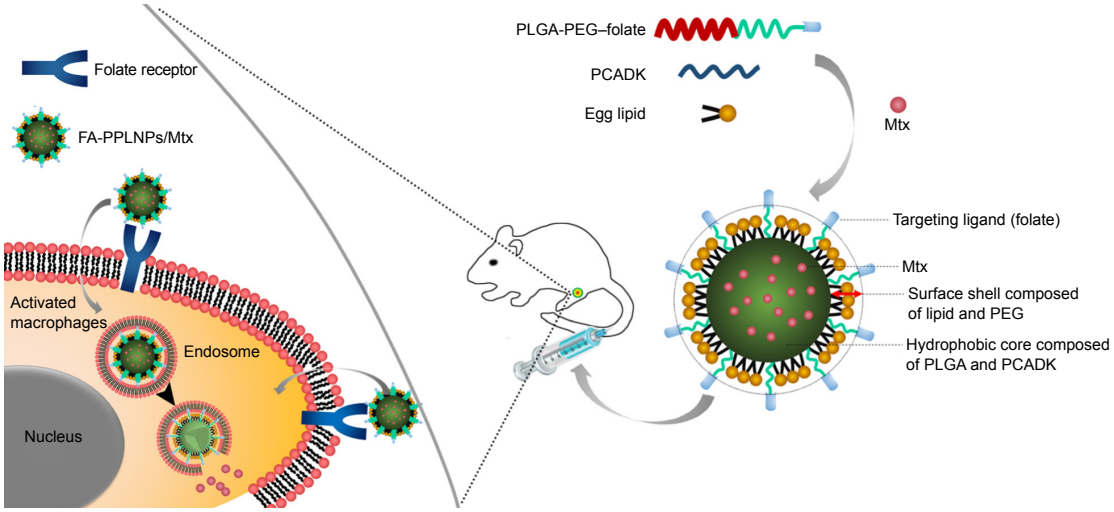

Scheme 1 Structure and mechanism of cellular uptake of FA-PPLNPs/Mtx.
Abbreviations: FA-PPLNPs/Mtx, methotrexate-loaded folic acid–polyethylene glycol–poly(lactic-*co*-glycolic acid)–poly(cyclohexane-1,4-diylacetone dimethylene ketal)–lipid nanoparticles; PCADK, poly(cyclohexane-1,4-diylacetone dimethylene ketal); PEG, polyethylene glycol; PLGA, poly(lactic-co-glycolic acid).

Due to increased vascular permeability associated with RA, LPNPs may be effective in drug delivery for this disease.[22,23] In order to deliver encapsulated drug to target tissues efficiently, efforts have been devoted to the development of intelligent delivery systems that respond to specific stimuli, such as pH level, temperature, and redox potential.[24–28] Among these are pH-responsive LPNPs, because the pH in inflammatory tissues (pH ~6.5), endosomes (pH ~5–6), and lysosomes (pH ~4–5) is significantly lower than that in blood circulation (pH ~7.4).[29,30] Poly(cyclohexane-1,4-diylacetone dimethylene ketal) (PCADK), a polyketal, is a promising material for constructing such drug carriers for inflammatory diseases and cancer, owing to its neutral degradation products and acid sensitivity.[31–34]

Herein, we report the development of multifunctional FRβ-targeting pH-responsive nanocarriers loaded with Mtx (Scheme 1). The nanocarriers were composed of poly(lactic-*co*-glycolic acid) (PLGA)–polyethylene glycol (PEG)–folic acid (FA), PCADK, and lipids (FA-PPLNPs). FA-PPLNPs were evaluated for their physicochemical properties and macrophage-targeting properties. Their in vivo efficacy was then evaluated in an adjuvant-induced arthritis (AIA) rat model.

Materials and methods

Materials

Mtx was purchased from Yuanye Biotechnology (Shanghai, China). PLGA was purchased from Boehringer Ingelheim Pharma (Ingelheim am Rhein, Germany). DMEM was purchased from Thermo Fisher Scientific (Waltham, MA, USA). Lipopolysaccharide (LPS) and polyvinyl alcohol (87%–89% hydrolyzed, molecular weight [MW] 13,000–23,000 Da) were purchased from Sigma-Aldrich (St Louis, MO, USA). fetal bovine serum (FBS) and RAW264.7 cells were obtained from Procell Biological Technology (Wuhan, China). 4′,6-diamidino-2-phenylindole (DAPI) was obtained from Beyotime Institute of Biotechnology (Haimen, China). Rhodamine B was obtained from Sinopharm Chemical Reagent (Shanghai, China). Acetonitrile was purchased from Thermo Fisher Scientific. MTT was obtained from Yuanye Biotechnology. Enzyme-linked immunosorbent assay (ELISA) kits for TNFα and IL6 were obtained from Elabscience Biotechnology (Wuhan, China). Complete Freund's adjuvant was obtained from Chondrex (Redmond, WA, USA). All chemicals used were of analytical grade and used without further purification.

Preparation of LPNPs

PCADK and FA-PEG-PLGA were synthesized as described previously.[35] Mtx-loaded FA-PPLNPs (FA-PPLNPs/Mtx) were prepared using modified emulsion–solvent evaporation. Briefly, PLGA, folate-PLGA-PEG, PCADK, and lipid were dissolved in 4 mL dichloromethane acetone solvent (1:1, v:v). Then, 5 mg Mtx was dissolved in the organic phase under sonication. The obtained organic phase containing Mtx was added slowly to 8 mL of 1% (w:v) polyvinyl alcohol (MW 30,000–70,000 Da, Sigma-Aldrich), and emulsified for 3 minutes by sonication in an ice bath at 100 W. The resulting emulsion was then added to 15 mL deionized water and evaporated under magnetic stirring at room temperature for 4 hours. The LPNPs obtained were pelleted by centrifugation (18,000 rpm, 15 minutes, 4°C) and washed three times with 30 mL deionized water. Rhodamine B-loaded LPNPs for

cell-uptake studies were prepared by the same method, except for replacing Mtx with rhodamine B. The resulting LPNPs were lyophilized for 24 hours and kept at 4°C until use. In the formulation design, polymer:lipid (w:w), PLGA:PCADK (w:w), and PLGA:FA-PEG-PLGA (w:w) were optimized to obtain the smallest particle size.

Characterization of LPNPs

The size and polydispersity index (PDI) of LPNPs were examined at 25°C by dynamic light scattering (DLS) using a Zetasizer Nano ZS90 from Malvern Instruments (Malvern, UK). Prior to measurement, LPNPs were reconstituted in deionized water at a concentration of 1 mg/mL and sonicated for 30 seconds.

Drug loading (DL) was determined by high-performance liquid chromatography (HPLC). Briefly, 2 mg LPNPs were dissolved in 200 µL dichloromethane. Then, 1 mL phosphate buffer solution (PBS) (0.1 M, pH 7.4) was added to extract the encapsulated Mtx. After centrifugation at 8,000 rpm for 10 minutes, the supernatant was collected and analyzed by HPLC. The HPLC system was equipped with Breeze software, a Waters 2,707 autosampler, a Waters 1,525 binary HPLC pump, and a Waters 2,487 ultraviolet-visible detector set at 302 nm. The sample was run on an Extend C_{18} column (4.6×250 mm, 5 µm) from Agilent Technologies (Santa Clara, CA, USA). The mobile phase consisted of 2% Na_2HPO4, 7% citric acid, and acetonitrile at a ratio of 80:10:10 (v:v:v). Flow rate and temperature were set at 1 mL/min and 27°C, respectively. Injection volume was 20 µL. DL and encapsulation efficiency (EE) were calculated thus:

$$\text{DL (\%)} = \frac{\text{Amount of drug encapsulated in LPNPs}}{\text{Amount of nanoparticles}} \times 100\%$$

$$\text{EE (\%)} = \frac{\text{Actual drug loading}}{\text{Theoretical drug loading}} \times 100\%$$

The average number of FA-PPLNPs/Mtx/mL of the nanosuspension (N) was determined using the equation:

$$N = \frac{6\,W \times 10^{-3}}{\pi\,(D \times 10^{-7})^3 \times \rho}$$

where W was the FA-PPLNP/Mtx concentration (mg/µL), D the particle diameter of FA-PPLNPs/Mtx, and ρ the FA-PPLNPs/Mtx density (weight per volume unit, estimated to be 0.82 g/cm^3 based on the density of the mixture of polymer and lipid).

The average number of folate molecules conjugated per milliliter in the same NP suspension (M) was calculated as:

$$M = \frac{K \times W \times 10^{-3} \times 6.02 \times 10^{23}}{MW}$$

where K was the ratio of FA-PLGA-PEG in FA-PPLNPs/Mtx (w:w, 13.5:50) and MW the MW of folate-PLGA-PEG. The average number of folate molecules conjugated per FA-PPLNPs/Mtx (surface density, P) was calculated as M/N. The distance (d) between two adjacent folate molecules was calculated with the following equation:

$$d = D\left(\frac{\pi}{P}\right)^{1/2}$$

FA-PPLNPs/Mtx were imaged by field-emission scanning electron microscopy on a JSM-6700F from JEOL (Tokyo, Japan). Briefly, FA-PPLNPs/Mtx suspension in water (1 mg/mL) was dropped on a silicon wafer and air-dried at room temperature. Then, samples were imaged using field-emission scanning electron microscopy at an accelerating voltage of 300 kV.

Stability of LPNPs

Lyophilized FA-PPLNPs/Mtx were suspended in deionized water, PBS (pH 7.4), and PBS with 10% FBS. LPNPs in different media were incubated at 37°C and 4°C. LPNP sizes and PDI were measured using DLS at predetermined time points to evaluate the stability of LPNPs.

Hemolysis tests

The hemocompatibility of FA-PPLNPs/Mtx and Mtx were analyzed as described previously.[36,37] Because the LPNPs were designed for intravenous injection, hemolysis analysis was used to determine their hemocompatibility. A fresh blood sample was drawn from the orbital sinus of a rat. Subsequently, red blood cells (RBCs) were isolated by centrifugation at 1,400× *g* for 15 minutes at 25°C. RBCs were washed with normal saline three times, followed by dilution to 2% (v:v). FA-PPLNPs/Mtx and Mtx were added to 2% RBCs in sterilized centrifuge tubes at different concentrations. The tubes were then incubated in a water bath at 37°C for 3 hours. Normal saline and 1% Triton X-100 were selected as the negative and positive controls, respectively. Further, RBC suspensions were centrifuged at 1,400× *g* for 15 minutes and supernatants collected. Aliquots of the supernatants (100 µL) were added to a 96-well plate and

further incubated for 30 minutes at room temperature. Free hemoglobin released from RBCs was determined at 540 nm. The hemolysis ratio was calculated thus:

$$\text{Hemolysis ratio (\%)} = \frac{A_{\text{sample}} - A_{\text{negative control}}}{A_{\text{positive control}} - A_{\text{negative control}}}$$

where A_{sample}, $A_{\text{negative control}}$, $A_{\text{positive control}}$ represent absorbance of samples, negative controls and positive controls, respectively.

In vitro release

Dialysis was performed to study the release kinetics of Mtx from the LPNPs. In brief, free Mtx (500 μg) or LPNPs (corresponding to 500 μg Mtx) were suspended in 2 mL dissolution medium (PBS pH 7.4 or 5) and sealed in dialysis bags with an MW cutoff of 10 kDa. The dialysis bags were then immersed in 10 mL PBS (pH 7.4 or 5) and incubated at 37°C in a shaker at 120 rpm. Concentrations of released Mtx were measured at predetermined time points by HPLC, as described earlier.

Cell cultures

RAW246.7 cells were cultured in DMEM containing 10% FBS at 37°C in a humidified atmosphere of 5% CO_2.

Cell-uptake studies

RAW246.7 cells were seeded in a 12-well plate at a density of 2×10^5 cells per well and activated with 1 μg/mL LPS for 48 hours.[38] Then, the medium was removed and replaced with an equal volume of growth medium containing rhodamine B-labeled LPNPs. The plate was incubated for an additional 2 hours. Then, cells were washed gently three times with PBS (0.01 M, pH 7.4) to remove residual LPNPs and fixed with 4% (w:v) formaldehyde in PBS for 20 minutes at room temperature. Subsequently, cellular nuclei were stained with DAPI (blue). Uptake of LPNPs by activated RAW264.7 cells was visualized using an LSM710 from Carl Zeiss Meditec (Jena, Germany).

Cytotoxicity assays

For cytotoxicity measurements, RAW246.7 cells were activated with 1 μg/mL LPS for 48 hours, seeded into a 96-well plate at a density of 10^4 cells per well, and incubated overnight. Then, the medium was replaced with medium containing various LPNPs or free Mtx at a series of Mtx concentrations. Then, cells were incubated for another 48 hours. Subsequently, 20 μL of MTT solution (5 mg/mL) was added and cells incubated for an additional 4 hours. Finally, the medium was discarded and formazan crystals formed from MTT conversion were dissolved with 150 μL dimethyl sulfoxide. Cell viability was determined by measuring absorbance at 490 nm on a plate reader. Relative cell viability was calculated thus:

$$\text{Cell viability} = \frac{A_{\text{sample}} - A_{\text{blank}}}{A_{\text{negative control}} - A_{\text{blank}}}$$

where A_{sample}, A_{blank}, $A_{\text{negative control}}$ represent absorbance of samples, blank, and negative control, respectively.

Establishment of a rat model of adjuvant-induced arthritis

Male Sprague Dawley rats were obtained from the experimental animal center of Jilin University, China. Animal experimental procedures were approved by the Experimental Animal Ethics Committee at the School of Life Sciences, Jilin University. All experiments on animals were performed according to Guidelines on Humane Treatment of Lab Animals, Jilin University (published in 2009). To generate the AIA rat model, 0.05 mL complete Freund's adjuvant was intradermally injected into the right footpad (day 0).

In vivo RA therapy and histological analysis

AIA rat models for therapy and histological analysis were established by the protocol described in the preceding section. On day 14 after induction, all rats were randomly divided into five groups consisting of five animals in each group: group 1, untreated AIA rats; group 2, normal control rats; groups 3–5, AIA rats treated with 0.5 mL Mtx solution, PPLNPs/Mtx, or FA-PPLNPs/Mtx in saline at an Mtx equivalent dose of 257 μg/kg body weight, every 2 days, intravenously. Rat paws were monitored and graded for severity: 0= normal, 1= slight swelling and confined erythema, 2= slight swelling and extended erythema, 3= moderate swelling and extended erythema, and 4= severe swelling and widespread erythema. After the final treatment, the thickness of the hind paws was also measured with a Vernier caliper. Subsequently, radiological examination was performed on affected paws with a Kodak FX Pro in vivo imaging system.

On day 19 after AIA induction, all rats were euthanized. For histological analysis, ankle joints were dissected and fixed in 10% (v:v) neutral formalin buffer for 24 hours and then decalcified in 10% (w:v) EDTA solution for three weeks at 37°C. Subsequently, ankle joints were embedded

in paraffin and sectioned (5 mm). Sections were stained with H&E and imaged on an Olympus microscope.

Biochemical analysis in serum

On day 19 after induction, rats were euthanized and serum samples collected. Serum levels of tumor necrosis factor (TNF) α and interleukin (IL)6 were determined using the ELISA kit from Elabscience Biotechnology following the manufacturer's instructions.

Statistical analysis

Data are expressed as mean ± SD. Statistical analysis of group differences was performed using one-way analysis of variance. $P<0.05$ was considered statistically significant.

Results and discussion

Preparation of LPNPs

We have previously demonstrated that drug delivery systems based on PCADK have pH sensitivity.[38] However, LPNPs and microspheres made of PCADK have rough surfaces and suboptimal drug-release behavior. Here, we used PLGA and PCADK to form polymeric cores of the LPNPs. Lipids were used to form a monolayer, acting as a shell. In addition, the LPNPs were PEGylated. Folate was covalently conjugated to PLGA via a PEG linker for targeting of FRβ-expressing activated macrophages. Several factors, including the polymer:lipid ratio (w:w), PLGA:PCADK ratio (w:w), and FA-PEG-PLGA:PLGA ratio (w:w), were investigated to obtain the smallest particle size. The particle size and PDI of different formulations are shown in Table 1. With decrease in polymer:lipid ratio from 10:0 to 5:5, particle size decreased significantly. Batch 3, which had the smallest particle size and PDI (156.5±4.94 nm, 0.138±0.028), was selected for further optimization. When the PLGA:PCADK ratio was decreased from 10:0 to 2:8, particle size changed from 148.8 nm to 183.5 nm and PDI changed from 0.138 to 0.414. When the PLGA:PCADK ratio was 5:5, LPNPs showed the smallest size and PDI (148.8 nm, 0.256). Finally, we partially replaced PLGA with FA-PEG-PLGA. Particle size decreased sharply with increased FA-PEG-PLGA:PLGA ratio. Based on these results, batch 14, in which the Mtx-loaded LPNPs were based on FA-PEG-PLGA, PCADK, and lipids (FA-PPLNPs/Mtx), was selected for evaluation in subsequent studies. LPNPs of batches 1, 3, and 7 were PNPs/Mtx, LPNPs/Mtx and PPLNPs/Mtx, respectively.

Characterization of LPNPs

As shown in Figure 1A, FA-PPLNPs/Mtx exhibited an average diameter of 133.6 nm and a narrow size distribution. FA-PPLNPs/Mtx were imaged by scanning electron microscopy (SEM). As shown in Figure 1C, LPNPs were relatively uniform in size and spherical. LPNP diameter determined by SEM (80–120 nm) was smaller than that determined by DLS (133.6 nm). This discrepancy could have been due to the fact that DLS was performed on LPNPs in deionized water, while SEM was on dehydrated LPNPs. The sizes of various LPNPs examined by DLS are shown in Figure 1D. The diameter of FA-PPLNPs was 133.6 nm, which was smaller than PNPs/Mtx (208.5 nm), LPNPs/Mtx (156.5 nm), and PPLNPs/Mtx (148.8 nm). Mtx was incorporated into FA-PPLNPs with DL of 2.35%.

The surface density of folate on FA-PPLNPs/Mtx was high. The distance between two neighboring folate molecules was 2.7 nm. This indicates that FA-PPLNPs/Mtx possessed

Table 1 Composition and characteristics of lipid–polymer nanoparticles

Batch	Polymer:lipid (w:w)	PLGA:PCADK (w:w)	FA-PEG-PLGA:PLGA (w:w)	Size (nm)	PDI
1	10:0	10:00	0:10	208.5±0.95	0.139±0.012
2	8:2		0:10	179±3.66	0.129±0.019
3	6:4		0:10	156.5±4.94	0.138±0.028
4	5:5		0:10	153.5±1.04	0.155±0.022
5	6:4	8:2	0:10	173.9±3.45	0.256±0.03
6		6:4	0:10	165.6±1.83	0.209±0.017
7		5:5	0:10	148.8±3.31	0.256±0.014
8		4:6	0:10	167.6±17.89	0.414±0.049
9		2:8	0:10	183.50±2.99	0.367±0.054
10	6:4	5:5	2:8	156.2±1.75	0.325±0.015
11			4:6	150.1±2.5	0.265±0.012
12			6:4	146.7±4.49	0.254±0.01
13			8:2	138.7±1.31	0.167±0.006
14			10:0	133.6±5.07	0.173±0.021

Note: Data are expressed as mean ± standard deviation.
Abbreviations: PLGA, poly(lactic-*co*-glycolic acid); PCADK, poly(cyclohexane-1,4-diylacetone dimethylene ketal); FA, folic acid; PEG, polyethylene glycol; PDI, polydispersity index.

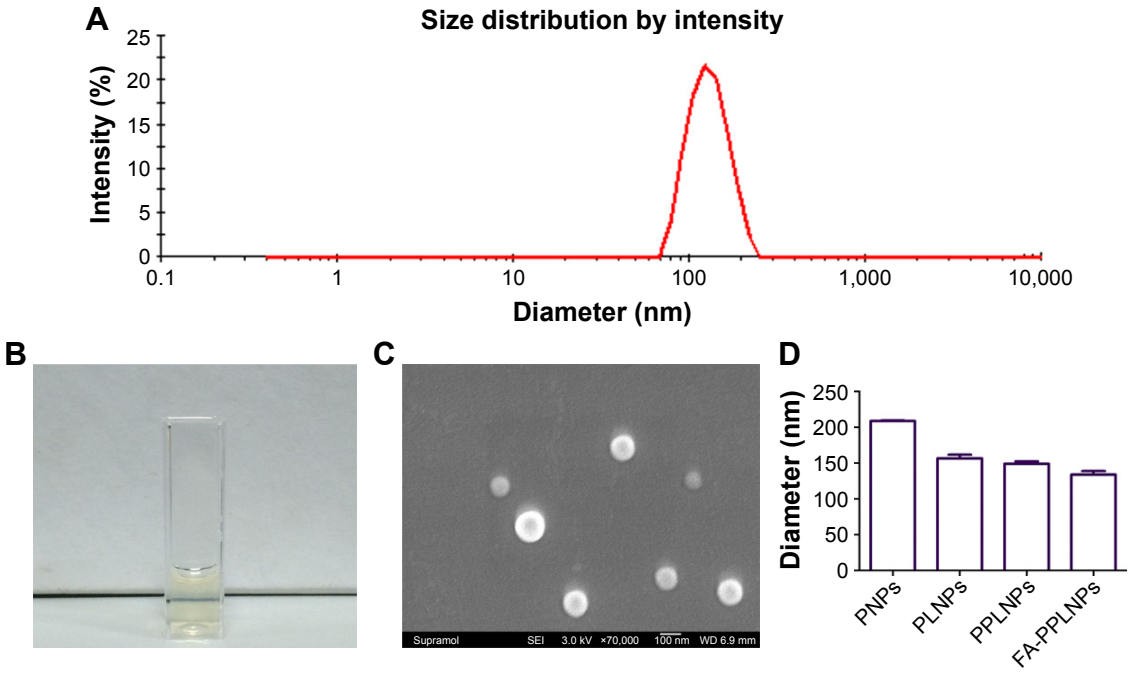

Figure 1 Characteristics of lipid–polymer NPs.
Notes: (**A**) Size distribution of FA-PPLNPs/Mtx based on DLS; (**B**) FA-PPLNPs/Mtx nanosuspension; (**C**) SEM images of FA-PPLNPs/Mtx; (**D**) hydrodynamic diameters of various NPs. Values are mean ± SD (n=3).
Abbreviations: NPs, nanoparticles; FA-PPLNPs/Mtx, methotrexate-loaded folic acid–polyethylene glycol–poly(lactic-*co*-glycolic acid)–poly(cyclohexane-1,4-diylacetone dimethylene ketal)–lipid NPs; DLS, dynamic light scattering; SEM, scanning electron microscopy; PNPs, poly(lactic-co-glycolic acid)-NPs; PLNPs, poly(lactic-co-glycolic acid)–lipid NPs.

abundant folate molecules on their surface, which should endow the LPNPs with high affinity for FRβ on activated macrophages.

Stability of LPNPs

To determine their stability, lyophilized LPNPs were resuspended in different media. As shown in Figure 2A and B, particle size and PDI did not change significantly in any media evaluated from days 0 to 5 at 4°C. From day 6 to day 7, particle size and PDI increased significantly in PBS with 10% FBS, which suggests particle aggregation. Nonetheless, these data support storage of LPNPs at 4°C in the absence of serum. Figure 2C and D show stability results of LPNPs in various media at 37°C. The size and PDI of LPNPs remained unchanged in all tested media during the first 2 days. From days 3 to 7, there was a sharp increase in size and PDI. These results showed that LPNPs were stable under physical temperature for 2 days. The LPNPs are likely stable in vivo, since they were likely fully distributed within the first 2 days after administration.

Hemolysis tests

Hemolysis tests were carried out to evaluate biocompatibility of the LPNPs. As shown in Figure 3, there was no significant hemolysis (<1%) when the concentration of Mtx increased from 1.56 to 100 μg/mL. This suggests that both FA-PPLNPs/Mtx and free Mtx possessed good biocompatibility upon intravenous administration.

In vitro release

The in vitro release profile of Mtx from FA-PPLNPs/Mtx was obtained in PBS at pH 7.4 and 5. As shown in Figure 4, there was burst release of Mtx from FA-PPLNPs/Mtx within the first hour, during which 14% and 35% of Mtx was released at pH 7.4 and 5, respectively. The burst release of Mtx from FA-PPLNPs/Mtx at pH 7.4 might have been caused by drug embedded in the surface or outer layer of the LPNPs. However, the burst release of Mtx at pH 5 was much greater, and indicates accelerated degradation of LPNPs at an acidic pH. In the following 5 hours (1–6 hours), the drug-release rate from FA-PPLNPs/Mtx was relatively constant. Approximately 35% and 62% of Mtx was released at pH 7.4 and 5, respectively. At pH 7.4, Mtx released from FA-PPLNPs/Mtx (64%) was significantly less than at pH 5 (81%). These results indicated high pH dependence for Mtx release from FA-PPLNPs/Mtx. Once FA-PPLNPs/Mtx reached an acidic environment, most of the encapsulated Mtx was released within a relatively short time.

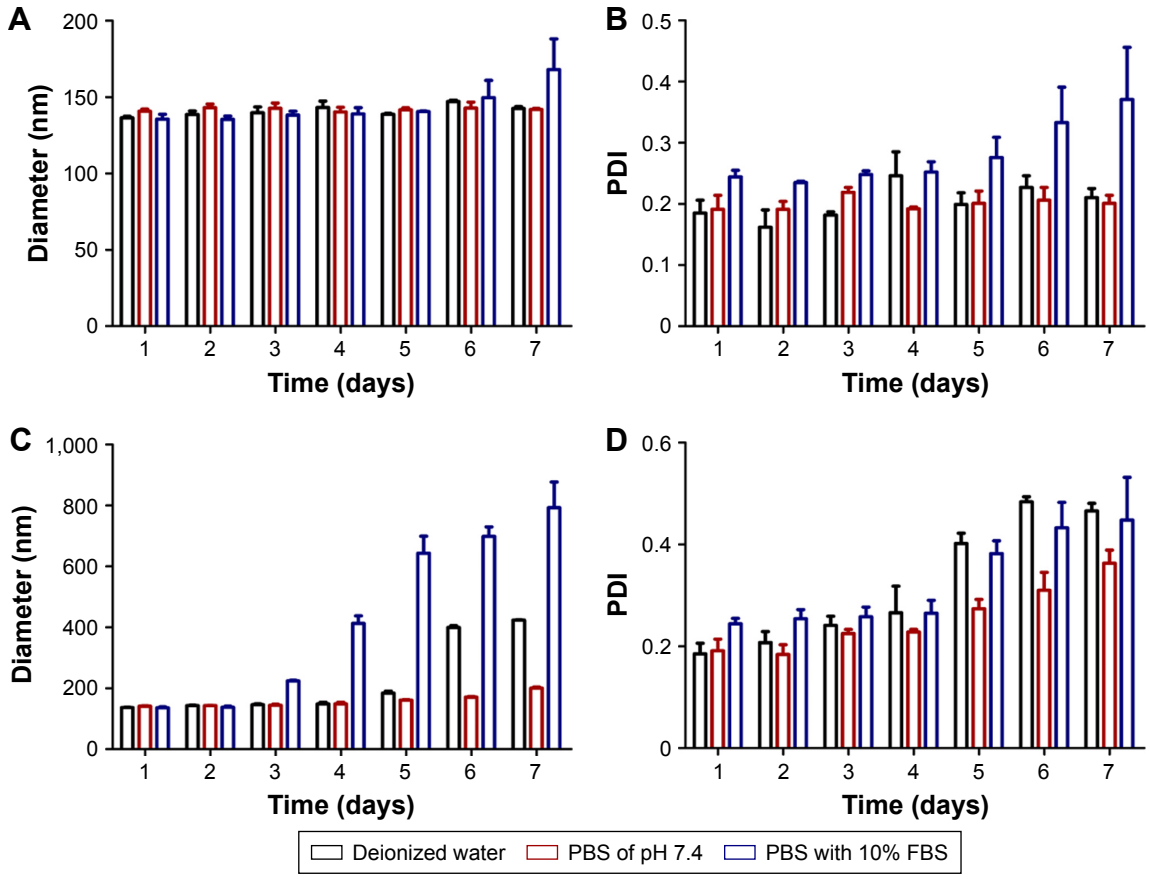

Figure 2 Colloidal stability of FA-PPLNPs/Mtx in different media.
Notes: Size and PDI were measured at 4°C (**A**, **B**) or 37°C (**C**, **D**). Values are mean ± SD (n=3).
Abbreviations: FA-PPLNPs/Mtx, methotrexate-loaded folic acid–polyethylene glycol–poly(lactic-*co*-glycolic acid)–poly(cyclohexane-1,4-diylacetone dimethylene ketal)–lipid nanoparticles; PDI, polydispersity index; FBS, fetal bovine serum.

Cell-uptake studies

FRβ has been shown to be overexpressed on activated macrophages. Activated macrophages are involved in inflammatory diseases, including RA, lupus, inflammatory osteoarthritis, and cancer. FA on the surface of LPNPs enables targeting of FRβ on inflammatory macrophages. To view the cellular uptake of FA-PPLNPs, loaded Mtx was replaced by rhodamine B. PPLNPs were used as a

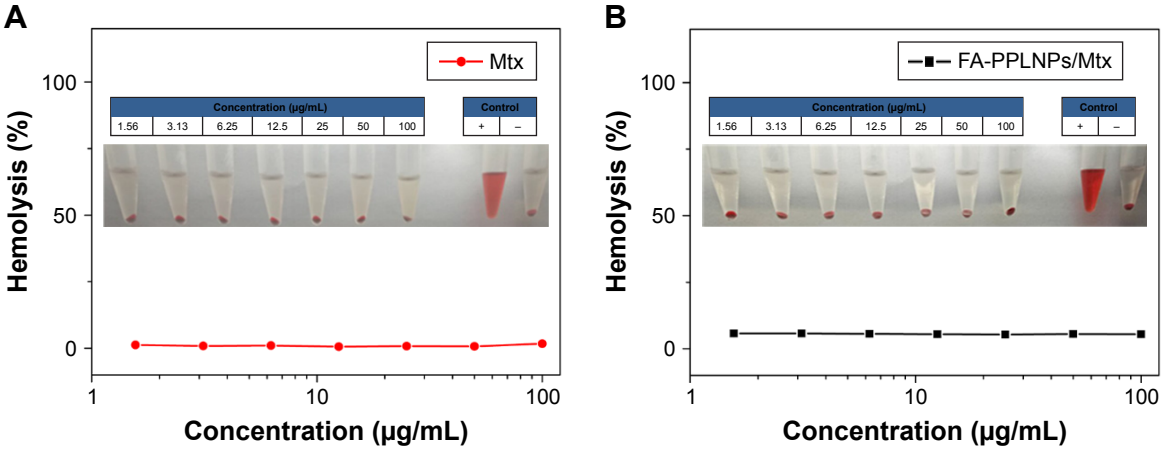

Figure 3 Hemolysis induction by lipid–polymer NP formulations.
Notes: Supernatants of red blood cells treated with free Mtx (**A**) and FA-PPLNPs/Mtx (**B**). Values are mean ± SD (n=6).
Abbreviation: FA-PPLNPs/Mtx, methotrexate-loaded folic acid–polyethylene glycol–poly(lactic-*co*-glycolic acid)–poly(cyclohexane-1,4-diylacetone dimethylene ketal)–lipid nanoparticles.

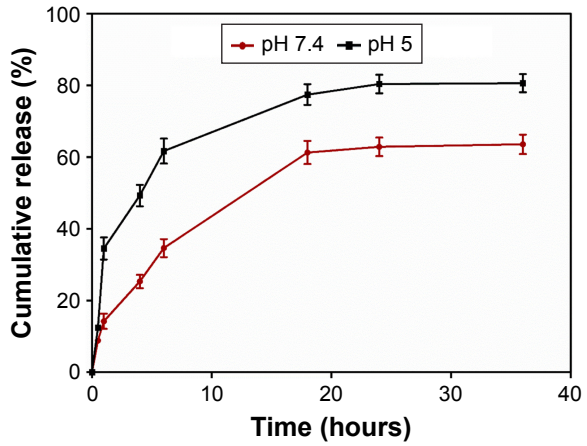

Figure 4 In vitro Mtx-release profiles from FA-PPLNPs/Mtx in PBS at pH 5 and pH 7.4 at 37°C. Values are mean ± SD (n=3).
Abbreviation: FA-PPLNPs/Mtx, methotrexate-loaded folic acid–polyethylene glycol–poly(lactic-*co*-glycolic acid)–poly(cyclohexane-1,4-diylacetone dimethylene ketal)–lipid nanoparticles; PBS, phosphate buffer solution.

negative control. As shown in Figure 5, the fluorescence intensity of rhodamine B in activated macrophages treated with FA-PPLNPs was markedly stronger than in the other three groups. The fluorescence intensity of rhodamine in non-activated macrophages treated with PPLNPs and FA-PPLNPs were barely detectable. These results indicated that LPS activation enhanced LPN uptake and FA actively targeted the FRs on the surface of activated macrophages.

Cytotoxicity assays

In vitro cytotoxicity of free Mtx, PPLNPs/Mtx, FA-PPLNPs/Mtx was measured using MTT assay. As shown in Figure 6A and B, blank FA-PPLNPs and blank PPLNPs had no significant cytotoxicity to activated RAW264.7 cells. Both the LPNP formulations and free Mtx displayed concentration-dependent cytotoxicity. PPLNPs and free Mtx exhibited similar cytotoxicity. However, the cytotoxicity of FA-PPLNPs/Mtx was significantly greater than that of PPLNPs/Mtx and free Mtx. The IC_{50} values of free Mtx, PPLNPs/Mtx, and FA-PPLNPs/Mtx were 0.0555, 0.0579, and 0.0159 μg/mL, respectively. The superior cytotoxicity of FA-PPLNPs/Mtx was likely caused by the active targeting of FRβ on the activated macrophages, consistent with the results of cellular uptake.

In vivo RA therapy

On day 14 after induction, RA was fully developed in the AIA rat model. Anti-inflammatory effects of the prepared LPNPs and free Mtx on the AIA rats were investigated by three methods: photographs of hind paws, measurement of paw thickness, and clinical scores of hind paws. As shown in Figure 7A, after the first treatment on day 14, clinical scores in all three groups decreased significantly. Rats treated with FA-PPLNPs/Mtx exhibited lower scores than rats treated

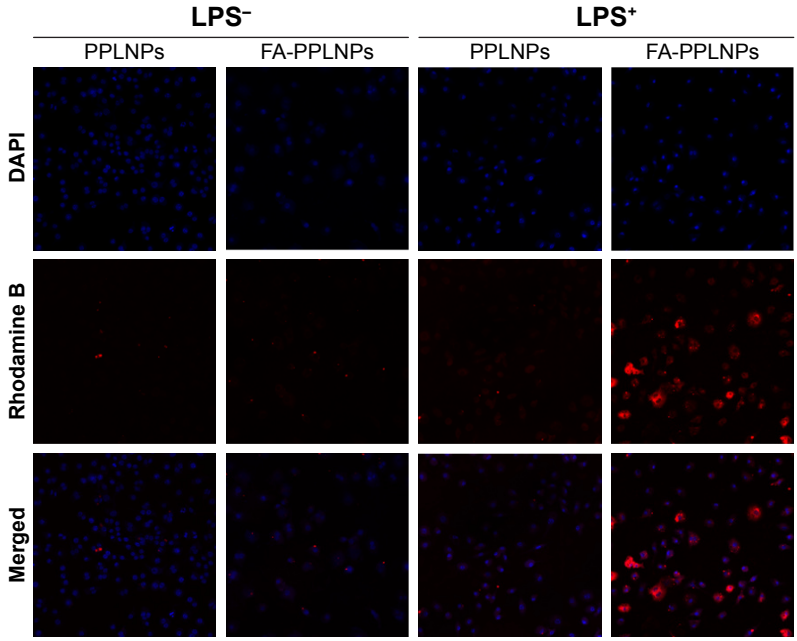

Figure 5 Cellular uptake of fluorescence-labeled lipid–polymer NPs.
Note: CLSM images show intracellular uptake of rhodamine B-labeled PPLNPs and FA-PPLNPs by RAW264.7 cells after activation by LPS (LPS^+) or not treated with LPS (LPS^-).
Abbreviations: CLSM, confocal laser-scanning microscopy; FA-PPLNPs, folic acid–polyethylene glycol–poly(lactic-*co*-glycolic acid)–poly(cyclohexane-1,4-diylacetone dimethylene ketone)–lipid nanoparticles; LPS, lipopolysaccharide; NPs, nanoparticles; DAPI, 4′,6-diamidino-2-phenylindole.

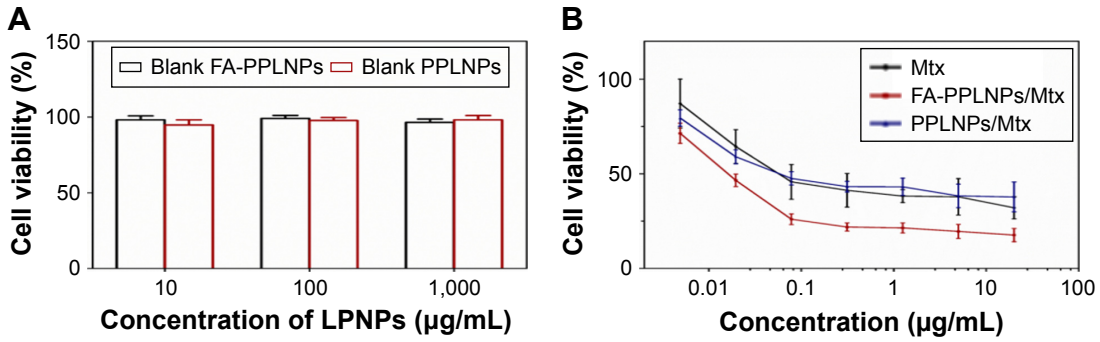

Figure 6 Cytotoxicity of lipid–polymer NPs.
Notes: RAW264.7 cells were activated by LPS and then treated with: (**A**) blank FA-PPLNPs and PPLNPs; (**B**) FA-PPLNPs/Mtx, PPLNPs/Mtx or free Mtx for 48 hours. Values are mean ± SD (n=6).
Abbreviation: FA-PPLNPs/Mtx, methotrexate-loaded folic acid–polyethylene glycol–poly(lactic-*co*-glycolic acid)–poly(cyclohexane-1,4-diylacetone dimethylene ketal)–lipid nanoparticles; LPS, lipopolysaccharide.

with PPLNPs/Mtx or free Mtx. However, after the second and third treatments, there were striking differences between the AIA rats treated with FA-PPLNPs/Mtx and those treated with PPLNPs/Mtx or free Mtx. On day 19, the average clinical score of the FA-PPLNPs/Mtx-treated group was reduced to 0.6, which was almost the same as the normal rats treated with saline.

All the rats tested were measured for paw thickness. In Figure 7B, remarkable difference in paw thickness was found between the FA-PPLNPs/Mtx-treated group and the

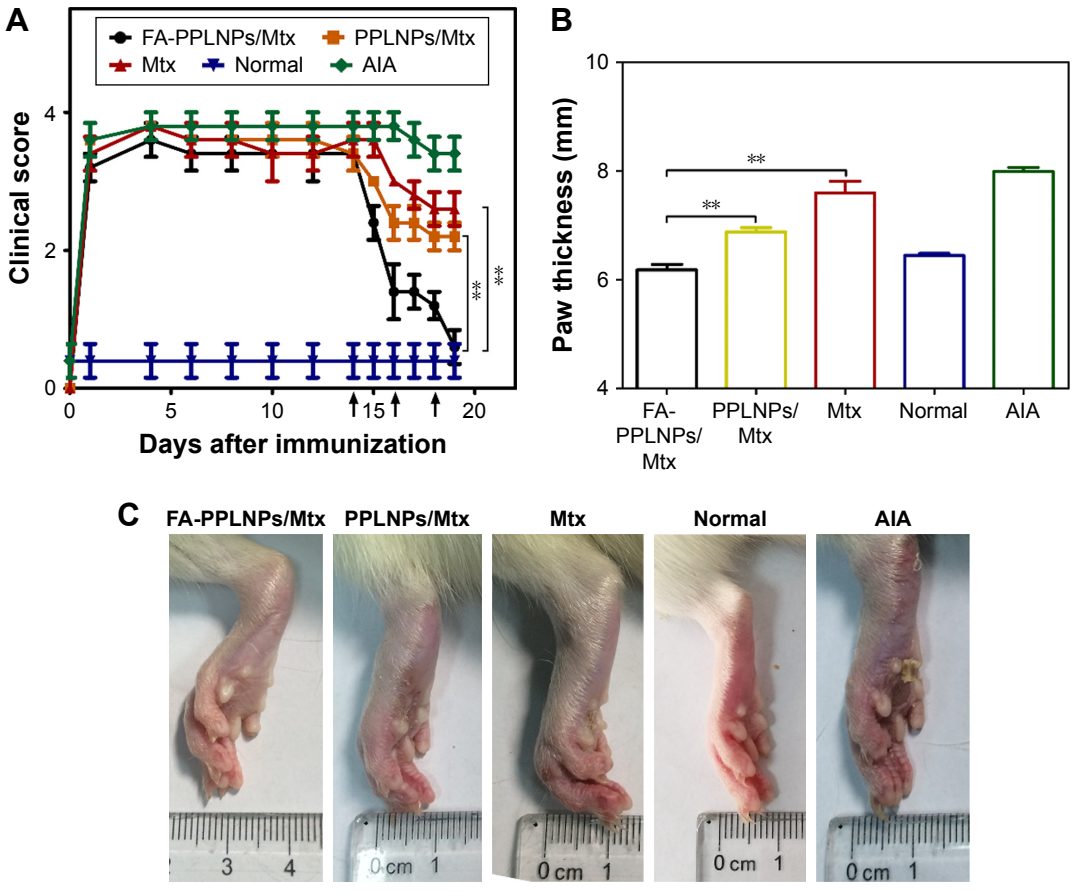

Figure 7 Therapeutic efficacy of FA-PPLNPs/Mtx, PPLNPs/Mtx, and free Mtx in AIA rats.
Notes: (**A**) Clinical scores of rheumatoid arthritis as a function of days after induction (arrows, FA-PPLNPs/Mtx, PPLNPs/Mtx, free Mtx, or saline); (**B**) paw thickness after all treatments, measured with caliper; (**C**) AIA rat paws from the different groups. Values are mean ± SD (n=5, $^{**}P<0.01$).
Abbreviations: FA-PPLNPs/Mtx, methotrexate-loaded folic acid–polyethylene glycol–poly(lactic-*co*-glycolic acid)–poly(cyclohexane-1,4-diylacetone dimethylene ketal)–lipid nanoparticles; AIA, adjuvant-induced arthritis.

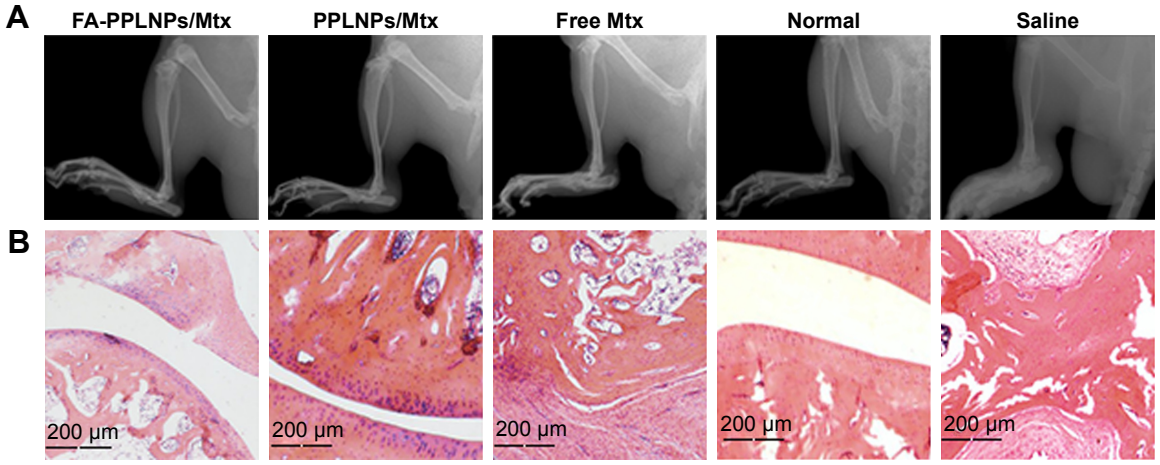

Figure 8 (**A**) Hind paws of AIA rats imaged by X-ray; (**B**) histological examination in ankle joints of normal rats and AIA rats treated with various formulations.
Abbreviations: AIA, adjuvant-induced arthritis; FA-PPLNPs/Mtx, methotrexate-loaded folic acid–polyethylene glycol–poly(lactic-*co*-glycolic acid)–poly(cyclohexane-1,4-diylacetone dimethylene ketal)–lipid nanoparticles.

other two groups ($P<0.01$ vs PPLNPs/Mtx, $P<0.001$ vs free Mtx). Paw thickness of rats treated with PPLNPs (6.18 mm) was similar to that of normal rats (6.45 mm). Figure 7C shows hind-paw images of all groups. Compared to normal rats treated with saline, paw swelling and erythema was seen in the free-Mtx solution-treated group and PPLNPs/Mtx-treated group. As for the FA-PPLNPs/Mtx-treated group, there was no visible paw swelling or erythema in the paws. These results indicate that FA-PPLNPs/Mtx could be a potent formulation in the treatment of RA. This may be due to FRβ targeting and the pH responsiveness of FA-PPLNPs/Mtx. Consistent with these results, radiography of the joints of AIA rats treated with FA-PPLNPs/Mtx revealed reduced bone destruction (Figure 8A).

Histological evaluation

Histological evaluation was performed on ankle joints. As expected, AIA rats treated with saline showed serious bone erosion, cartilage destruction, and synovial hyperplasia. Meanwhile, extensive histopathology made it difficult to identify joint space. In contrast, AIA rats treated with FA-PPLNPs/Mtx showed smooth articulation of the cartilage surface, negligible bone erosion, and synovial hyperplasia (Figure 8B).

Biochemical analysis in serum

In RA, levels of proinflammatory cytokines secreted by macrophages are associated with disease progression. These include TNFα and IL6.[40] Levels of TNFα and IL6 in serum were measured by ELISA. As shown in Figure 9, AIA rats

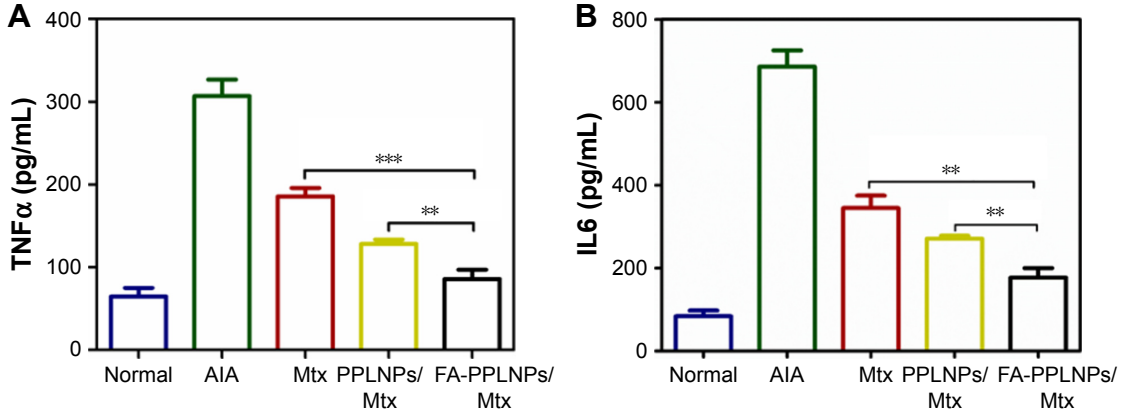

Figure 9 Serum concentrations.
Notes: TNFα (**A**) and IL6 (**B**) from normal rats and AIA rats treated with Mtx solution, PPLNPs/Mtx, and FA-PPLNPs/Mtx. Values are mean ± SD (n=3, $^{**}P<0.01$, $^{***}P<0.001$).
Abbreviations: AIA, adjuvant-induced arthritis; FA-PPLNPs/Mtx, methotrexate-loaded folic acid–polyethylene glycol–poly(lactic-*co*-glycolic acid)–poly(cyclohexane-1,4-diylacetone dimethylene ketal)–lipid nanoparticles; IL, interleukin; TNFα, tumor necrosis factor α.

treated with saline exhibited elevated levels of TNFα and IL6. However, in the three groups individually treated with FA-PPLNPs/Mtx, PPLNPs/Mtx, and free Mtx, TNFα and IL6 levels decreased to different degrees.

Conclusion

FRβ-targeting and pH-responsive FA-PPLNPs/Mtx were developed for the treatment of RA. These had small particles with narrow distribution. In vitro release studies indicated FA-PPLNPs/Mtx exhibited excellent pH-responsiveness with accelerated drug release at acidic pH. Cellular uptake and cytotoxicity assays implied that FA on the surface of FA-PPLNPs/Mtx bound to FRβ on activated macrophages, which resulted in greater inhibition of cell proliferation. Importantly, the results of in vivo therapy and histological analysis showed that treatment with FA-PPLNPs/Mtx significantly reduced the progression of RA in AIA rats. Together, these results indicate that FA-PPLNPs/Mtx is a promising novel therapeutic for the treatment of RA.

Acknowledgment

We thank Guodong Yan at Jilin University for advice and assistance in generating the X-ray imaging data.

Disclosure

The authors report no conflicts of interest in this work.

References

1. Firestein GS. Evolving concepts of rheumatoid arthritis. *Nature*. 2003;423(6937):356–361.
2. Moura CC, Segundo MA, das Neves J, Reis S, Sarmento B. Co-association of methotrexate and SPIONs into anti-CD64 antibody-conjugated PLGA nanoparticles for theranostic application. *Int J Nanomedicine*. 2014;9:4911–4922.
3. Smolen JS, Steiner G. Therapeutic strategies for rheumatoid arthritis. *Nat Rev Drug Discov*. 2003;2(6):473–488.
4. Kim YJ, Chae SY, Jin CH, et al. Ionic complex systems based on hyaluronic acid and PEGylated TNF-related apoptosis-inducing ligand for treatment of rheumatoid arthritis. *Biomaterials*. 2010;31(34):9057–9064.
5. Burmester GR, Stuhlmüller B, Keyszer G, Kinne RW. Mononuclear phagocytes and rheumatoid synovitis: mastermind or workhorse in arthritis? *Arthritis Rheum*. 1997;40(1):5–18.
6. Kim SH, Kim JH, You DG, et al. Self-assembled dextran sulphate nanoparticles for targeting rheumatoid arthritis. *Chem Commun (Camb)*. 2013;49(88):10349–10351.
7. Kinne RW, Stuhlmüller B, Burmester GR. Cells of the synovium in rheumatoid arthritis: macrophages. *Arthritis Res Ther*. 2007;9(6):224.
8. Low PS, Henne WA, Doorneweerd DD. Discovery and development of folic-acid-based receptor targeting for Imaging and therapy of cancer and inflammatory diseases. *Acc Chem Res*. 2008;41(1):120–129.
9. Smolen JS, Landewé R, Breedveld FC, et al. EULAR recommendations for the management of rheumatoid arthritis with synthetic and biological disease-modifying antirheumatic drugs: 2013 update. *Ann Rheum Dis*. 2014;73(3):492–509.
10. Braun J, Rau R. An update on methotrexate. *Curr Opin Rheumatol*. 2009;21(3):216–223.
11. Ranganathan P. An update on methotrexate pharmacogenetics in rheumatoid arthritis. *Pharmacogenomics*. 2008;9(4):439–451.
12. Favalli EG, Biggioggero M, Meroni PL. Methotrexate for the treatment of rheumatoid arthritis in the biologic era: still an "anchor" drug? *Autoimmun Rev*. 2014;13(11):1102–1108.
13. Nogueira E, Lager F, Le Roux D, et al. Enhancing methotrexate tolerance with folate tagged liposomes in arthritic mice. *J Biomed Nanotechnol*. 2015;11(12):2243–2252.
14. Khan ZA, Tripathi R, Mishra B. Methotrexate: a detailed review on drug delivery and clinical aspects. *Expert Opin Drug Deliv*. 2012;9(2):151–169.
15. Alibolandi M, Abnous K, Sadeghi F, Hosseinkhani H, Ramezani M, Hadizadeh F. Folate receptor-targeted multimodal polymersomes for delivery of quantum dots and doxorubicin to breast adenocarcinoma: In vitro and in vivo evaluation. *Int J Pharm*. 2016;500(1–2):162–178.
16. Xie J, Yang ZG, Zhou CG, Zhu J, Lee RJ, Teng L. Nanotechnology for the delivery of phytochemicals in cancer therapy. *Biotechnol Adv*. 2016;34(4):343–353.
17. Garg NK, Singh B, Sharma G, et al. Development and characterization of single step self-assembled lipid polymer hybrid nanoparticles for effective delivery of methotrexate. *RSC Adv*. 2015;5(77):62989–62999.
18. Zhang LF, Chan JM, Gu FX, et al. Self-assembled lipid-polymer hybrid nanoparticles: a robust drug delivery platform. *ACS Nano*. 2008;2(8):1696–1702.
19. Mandal B, Bhattacharjee H, Mittal N, et al. Core-shell-type lipid-polymer hybrid nanoparticles as a drug delivery platform. *Nanomedicine*. 2013;9(4):474–491.
20. Hadinoto K, Sundaresan A, Cheow WS. Lipid-polymer hybrid nanoparticles as a new generation therapeutic delivery platform: a review. *Eur J Pharm Biopharm*. 2013;85(3):427–443.
21. Li YH, Lee RJ, Yu KT, et al. Delivery of siRNA using lipid nanoparticles modified with cell penetrating peptide. *ACS Appl Mater Interfaces*. 2016;8(40):26613–26621.
22. Koch AE. Angiogenesis as a target in rheumatoid arthritis. *Annals Of the Rheumatic Diseases*. 2003;62 Suppl 2:ii60–ii67.
23. Heo R, Park JS, Jang HJ, et al. Hyaluronan nanoparticles bearing γ-secretase inhibitor: in vivo therapeutic effects on rheumatoid arthritis. *J Control Release*. 2014;192:295–300.
24. Chen HC, Liu DY, Guo ZJ. Endogenous stimuli-responsive nanocarriers for drug delivery. *Chem Lett*. 2016;45(3):242–249.
25. Chen CY, Kim TH, Wu WC, et al. pH-dependent, thermosensitive polymeric nanocarriers for drug delivery to solid tumors. *Biomaterials*. 2013;34(18):4501–4509.
26. Mura S, Nicolas J, Couvreur P. Stimuli-responsive nanocarriers for drug delivery. *Nat Mater*. 2013;12(11):991–1003.
27. Bae Y, Nishiyama N, Fukushima S, Koyama H, Yasuhiro M, Kataoka K. Preparation and biological characterization of polymeric micelle drug carriers with intracellular pH-triggered drug release property: tumor permeability, controlled subcellular drug distribution, and enhanced in vivo antitumor efficacy. *Bioconjug Chem*. 2005;16(1):122–130.
28. Hu YX, Haynes MT, Wang YH, Liu F, Huang L. A highly efficient synthetic vector: nonhydrodynamic delivery of DNA to hepatocyte nuclei in vivo. *ACS Nano*. 2013;7(6):5376–5384.
29. Ganta S, Devalapally H, Shahiwala A, Amiji M. A review of stimuli-responsive nanocarriers for drug and gene delivery. *J Control Release*. 2008;126(3):187–204.
30. Mura S, Nicolas J, Couvreur P. Stimuli-responsive nanocarriers for drug delivery. *Nat Mater*. 2013;12(11):991–1003.
31. Lee S, Yang SC, Heffernan MJ, Taylor WR, Murthy N. Polyketal microparticles: a new delivery vehicle for superoxide dismutase. *Bioconjug Chem*. 2007;18(1):4–7.
32. Lee SM, Yang SC, Kao CY, Pierce RH, Murthy N. Solid polymeric microparticles enhance the delivery of siRNA to macrophages in vivo. *Nucleic Acids Res*. 2009;37(22):e145.

33. Yang SC, Bhide M, Crispe IN, Pierce RH, Murthy N. Polyketal copolymers: a new acid-sensitive delivery vehicle for treating acute inflammatory diseases. *Bioconjug Chem*. 2008;19(6):1164–1169.
34. Sy JC, Phelps EA, García AJ, Murthy N, Davis ME. Surface functionalization of polyketal microparticles with nitrilotriacetic acid-nickel complexes for efficient protein capture and delivery. *Biomaterials*. 2010;31(18):4987–4994.
35. Sy JC, Seshadri G, Yang SC, et al. Sustained release of a p38 inhibitor from non-inflammatory microspheres inhibits cardiac dysfunction. *Nat Mater*. 2008;7(11):863–869.
36. Vijayakumar MR, Kosuru R, Singh SK, et al. Resveratrol loaded PLGA: D-α-tocopheryl polyethylene glycol 1000 succinate blend nanoparticles for brain cancer therapy. *RSC Adv*. 2016;6(78):74254–74268.
37. Yang M, Ding J, Zhang Y, et al. Activated macrophage-targeted dextran-methotrexate/folate conjugate prevents deterioration of collagen-induced arthritis in mice. *J Mater Chem B*. 2016;4(12):2102–2113.
38. Wang Q, Jiang JY, Chen WF, Jiang H, Zhang ZR, Sun X. Targeted delivery of low-dose dexamethasone using PCL-PEG micelles for effective treatment of rheumatoid arthritis. *J Control Release*. 2016;230:64–72.
39. Wang CH, Yu CH, Liu JX, et al. Preparation and in vivo evaluation of PCADK/PLGA microspheres for improving stability and efficacy of rhGH. *Int J Pharm*. 2015;495(2):924–931.
40. Roy K, Kanwar RK, Kanwar JR. Molecular targets in arthritis and recent trends in nanotherapy. *Int J Nanomedicine*. 2015;10:5407–5420.